Applied Physics Letters

The effects of strain relaxation on the dielectric properties of epitaxial ferroelectric $Pb(Zr_{0.2}Ti_{0.8})TiO_3$ thin films

Cite as: Appl. Phys. Lett. **105**, 022903 (2014); https://doi.org/10.1063/1.4885551
Submitted: 02 June 2014 • Accepted: 16 June 2014 • Published Online: 14 July 2014

Asif Islam Khan, Pu Yu, Morgan Trassin, et al.

View Online

Export Citation

CrossMark

ARTICLES YOU MAY BE INTERESTED IN

Ferroelectric thin films: Review of materials, properties, and applications
Journal of Applied Physics **100**, 051606 (2006); https://doi.org/10.1063/1.2336999

Ferroelectricity in hafnium oxide thin films
Applied Physics Letters **99**, 102903 (2011); https://doi.org/10.1063/1.3634052

AlScN: A III-V semiconductor based ferroelectric
Journal of Applied Physics **125**, 114103 (2019); https://doi.org/10.1063/1.5084945

Time to get excited.
Lock-in Amplifiers – from DC to 8.5 GHz
Find out more
Zurich Instruments

AIP Publishing

© 2014 AIP Publishing LLC.

The effects of strain relaxation on the dielectric properties of epitaxial ferroelectric $Pb(Zr_{0.2}Ti_{0.8})TiO_3$ thin films

Asif Islam Khan,[1,a)] Pu Yu,[2,b)] Morgan Trassin,[2,c)] Michelle J. Lee,[3,b)] Long You,[1] and Sayeef Salahuddin[1]

[1]*Department of Electrical Engineering and Computer Sciences, University of California, Berkeley, California 94720, USA*
[2]*Department of Physics, University of California, Berkeley, California 94720, USA*
[3]*Department of Material Science and Engineering, University of California, Berkeley, California 94720, USA*

(Received 2 June 2014; accepted 16 June 2014; published online 14 July 2014)

We study the effects of strain relaxation on the dielectric properties of epitaxial 40 nm $Pb(Zr_{0.2}Ti_{0.8})TiO_3$ (PZT) films. A significant increase in the defect and dislocation density due to strain relaxation is observed in PZT films with tetragonality $c/a < 1.07$ grown on $SrTiO_3$ (001) substrates, which results in significant frequency dispersion of the dielectric constant and strong Rayleigh type behavior in those samples. This combined structural-electrical study provides a framework for investigating strain relaxation in thin films and can provide useful insights into the mechanisms of fatigue in ferroelectric materials. © *2014 AIP Publishing LLC.*
[http://dx.doi.org/10.1063/1.4885551]

Epitaxial strain engineering on ferroelectric thin film can significantly enhance their properties, which opens the door to many new applications and novel functionalities.[1–5] Strain is generally imparted on a thin film by epitaxially growing the material on a substrate which has in-plane lattice parameters different than those of the material. For all practical purposes, epitaxial strain is strongly affected by the thermodynamic and/or kinetic processes during the growth,[6] and therefore, strain relaxation can take place at different stages of the thin film deposition, leading to a ferroelectric oxide that is partially or fully relaxed. Strain relaxation has also been shown to occur during fatigue in epitaxially strained ferroelectric thin films.[7] Microscopic details of strain relaxation and their impact on the overall properties in ferroelectric thin films have been reported in the literature.[8–13]

One of the most dominant factors in determining the epitaxial strain in the film thickness. Gradual relaxation of strain with increasing thickness in epitaxial $Pb(Zr_{0.2}Ti_{0.8})TiO_3$ (PZT) thin films was previously studied in Refs. 14 and 15. However, variations in growth conditions could also lead to varying strain for the same thickness.[16,17] Therefore, by studying films with the same thickness but varying degree of strain relaxation, it is possible to gain insights into parameters other than thickness that can lead to strain relaxation. In this work, we do that by studying the effects of strain relaxation on the dielectric response of $Pb(Zr_{0.2}Ti_{0.8})TiO_3$ films of the same thickness (40 nm). We show that defects and dislocations introduced due to the relaxation of strain strongly affect the dielectric properties of the ferroelectric films and result in a large frequency dispersion of the dielectric constant and a strong Rayleigh type behavior in relaxed films. Furthermore, we correlate the electrical properties with the macroscopic structural parameters such as the tetragonality.

$Pb(Zr_{0.2}Ti_{0.8})O_3$ is a highly polar ferroelectric with a tetragonal perovskite structure (space group $P4mm$). Among different stoichiometric variants of $Pb(Zr_xTi_{1-x})O_3$, $Pb(Zr_{0.2}Ti_{0.8})O_3$ has one of the largest values of the remnant polarization ($\sim$80 μC/cm^2).[14] $Pb(Zr_{0.2}Ti_{0.8})O_3$ is found to be ferroelectric even at a thickness of 5 nm (Ref. 18) and is an important candidate for non-volatile memory applications as well as micro-electro-mechanical systems.[19,20] We grew 40 nm PZT films on $SrRuO_3$ (SRO) buffered $SrTiO_3$ (STO) (001) and $DyScO_3$ (DSO) (110) substrates using the pulsed laser deposition (PLD) technique. The in-plane lattice parameter of the STO (001) substrate, a_{STO}, is 3.905 Å, which imposes a compressive strain ($\epsilon_{STO} = -0.65\%$) on the PZT film. On the other hand, the DSO (110) pseudo-cubic template ($a_{DSO} = 3.945$ Å) imposes a tensile strain ($\epsilon_{DSO} = +0.33\%$) on PZT films. Piezo-response force microscopy confirms that our 40 nm PZT films grown on both STO and DSO are monodomain with the PZT c-axis oriented along the out-of-the-plane direction (results not shown). We grew SRO and PZT layers at 630 °C and 720 °C, respectively. During the growth, the oxygen partial pressure was kept at 100 mTorr, and afterwards, the heterostructures were slowly cooled down at a rate of -5 °C/min to the room temperature at 1 atm partial pressure of oxygen. Laser pulses with 100 mJ energy and $\sim$4 mm^2 spot size were used to ablate the targets. Gold top electrodes were fabricated afterwards by standard microfabrication techniques. The structural properties of the heterostructures were investigated by X-ray diffraction (XRD) technique to evaluate the lattice parameters, strain state, and crystalline quality. A PANalytical X'Pert PRO Materials Research Diffractometer (MRD) was used to obtain standard $\theta - 2\theta$ and ω spectra and the reciprocal space maps (RSMs). Figs. 1(a) and 1(b) show the RSMs of strained PZT films (40 nm) grown on SRO buffered STO and DSO substrates, respectively, around (103)

a)Electronic mail: asif@eecs.berkeley.edu
b)Present address: Department of Physics, Tsinghua University, Beijing, China.
c)Present address: Department of Materials, ETH Zurich, Wolfgang-Pauli Strasse 10, CH-8093 Zurich, Switzerland.

 © 2014 AIP Publishing LLC

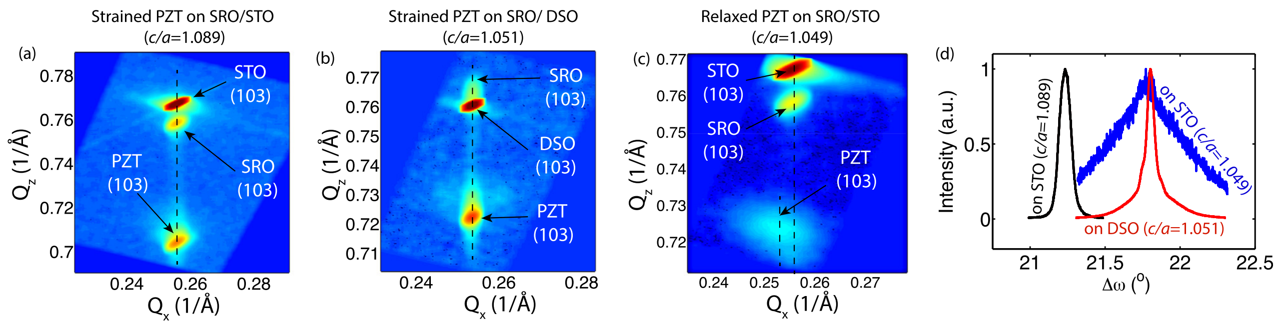

FIG. 1. (a)–(c) Reciprocal space maps around (103) peaks of strained PZT films grown on SRO buffered STO (a) and DSO (b) substrates and a relaxed PZT film grown on SRO buffered STO substrate (c). (d) FWHM around the PZT (002) peak calculated from X-ray diffraction spectrum rocking curve measurements on strained and relaxed PZT films.

peaks. We note in Figs. 1(a) and 1(b) that the (103) peaks of PZT, SRO, and substrate align along a constant Q_x line confirming that, within the resolution limit of the X-ray diffractometer, there is no observable relaxation of the epitaxial strain in the PZT and the SRO layers. The average PZT c-axis lattice parameter and the tetragonality (c/a) of the strained PZT films grown on STO and DSO are {4.253 Å and 1.089} and {4.14 Å and 1.051}, respectively. This observation is in agreement with the fact that as the substrate is changed from DSO to STO, the increasing compressive strain (or decreasing tensile strain) results in the elongation of the PZT unit cell along the c-axis direction. Fig. 1(c) shows the reciprocal space map of a relaxed 40 nm PZT film grown on SRO buffered STO substrate around (103) peaks. We observe in Fig. 1(c) that the PZT (103) peak occurs at a smaller Q_x than the STO (103) peak in this sample indicating that the PZT layer is not epitaxially coherent to the substrate. Fig. 1(d) shows the rocking curve measurements around the PZT (002) peaks in these three samples. We observe in Fig. 1(d) that the relaxed PZT film has a full-width-at-half-maximum (FWHM) much larger than those for both of the other two strained PZT films. The FWHM is a measure of the crystalline quality of a film. The relaxation of strain in thin films generally occurs through the formation of misfit dislocations. These misfit dislocations are generally located at the interface between SRO and PZT layers,[8,10,13] which results in a significant distortion of local strain field, thereby degrading the crystalline quality and increasing the FWHM. Using X-ray micro diffraction techniques on 30 nm $Pb(Zr_{0.3}Ti_{0.7})O_3$ films grown on SRO buffered STO (001) substrates, Do *et al.*[7] showed that, in the regions of the ferroelectric film where a significant relaxation of strain occurs, the $Pb(Zr_{0.3}Ti_{0.7})O_3$ (002) reflection becomes broader in rocking curve measurements and the out-of-plane lattice parameter decreases by 0.3%, which are in agreement with our observations.

We indeed observed that, even when 40 nm PZT films were grown directly on STO substrates without SRO buffer layers, the tetragonality of PZT films obtained from different growth runs varied in the range of 1.045–1.09. In order to understand this variation, we note that the strain relaxation length of PZT on STO, $l_{PZT-STO}$, was reported to be ∼40 nm.[14] In epitaxial growth processes, as the film thickness approaches the strain relaxation length, minute alteration of the kinetics caused by the slight variations of PLD process parameters (such as the growth pressure and temperature, laser energy per pulse, and cooling rate) might often cause the epitaxial strain to relax.[17] Hence, we attribute this variation of the strain state (strained or relaxed) in our 40 nm PZT films on STO to the minute variations of our PLD parameters, which are stochastic in nature. We did not observe such variations in the lattice parameters of our $Pb(Zr_{0.2}Ti_{0.8})O_3$ films thicker than 80 nm grown on STO substrates, and the c-axis lattice parameter and c/a of those thick films were found to be ∼4.14 Å and ∼1.045 (results not shown). This indicates that thicker PZT films (>80 nm) are relaxed and the strain state in those thick films is not sensitive the stochastic variations in the growth conditions. We also note that the tetragonality of 40 nm PZT films on STO reported by different groups lies in the range of 1.045–1.09 (for example, $c/a = 1.045$,[15] 1.087,[14] and 1.075[18]). Furthermore, due to the smaller lattice mismatch between PZT and DSO, the strain relaxation length of PZT on DSO, $l_{PZT-DSO}$, is expected to be much larger than $l_{PZT-STO}$ (=40 nm). As a result, the strain state of 40 nm PZT films grown under nominally same conditions on DSO is expected to be significantly less sensitive to stochastic variations of the PLD parameters and, indeed, we did not observe any significant variation in the lattice parameters of PZT films grown on DSO substrates. These observations indicate that the high sensitivity of the growth kinetics of films with thicknesses close to the strain relaxation length to the PLD process parameters results in a significant variation of the strain state of our 40 nm PZT films grown on STO substrates.

Fig. 2 plots the FWHM around the PZT (002) peak of a set of PZT films grown on SRO buffered STO and DSO

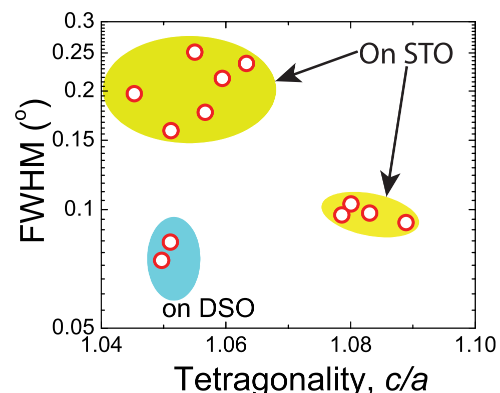

FIG. 2. FWHM around PZT (002) peaks as a function of tetragonality (c/a) for PZT/SRO heterostructures grown on STO and DSO substrates.

substrates as a function of PZT c/a. In Fig. 2, we observe that the PZT films on STO with c/a in the range 1.07–1.089 consistently show a narrower FWHM (FWHM $\leq \sim 0.1°$) than those of the samples with c/a in the range of 1.045–1.007 (FWHM $\geq \sim 0.15°$). This suggests that there is a significant increase in the defect and dislocation density as c/a of PZT grown on STO goes below 1.07. We also note in Fig. 2 that 40 nm PZT films grown on DSO substrates consistently show FWHM $\leq 0.1°$. This rules out the possibility that there might be an intrinsic connection between the c/a value and the FWHM.

Now, we compare the dielectric properties of strained and relaxed PZT films. Capacitance measurements were performed using an HP 4194A Impedance/Gain-Phase Analyzer. Fig. 3(a) shows the dielectric constant ε_r of the PZT films as a function of the electric field at 100 kHz. We refer to the cross point of the up- and the down-sweep of the ε_r-electric field curves as the nominal ε_r of a sample. Figs. 3(b) and 3(c) show the frequency dispersion of the dielectric constant of the samples. In Fig. 3(c), the dielectric constant is scaled with respect to the dielectric constant of the respective sample at 1 MHz. Both of the strained samples on STO and DSO show a frequency dispersion $((\varepsilon_{r,10\ \mathrm{kHz}} - \varepsilon_{r,1\ \mathrm{MHz}})/\varepsilon_{r,1\ \mathrm{MHz}})$ of $\sim$4%, whereas the relaxed sample on STO shows a frequency dispersion of $\sim$12%. Fig. 3(d) shows the frequency dispersion as a function of the tetragonality, c/a. Fig. 3(d) clearly shows that there is a drastic increase in the frequency dispersion as c/a of PZT films grown on STO decreases below 1.07. The frequency dispersion of ε_r is usually attributed to the extrinsic mechanisms such as defects and dislocations in insulating thin films. This aforementioned trend of frequency dispersion underpins the fact that the extrinsic mechanisms become more dominant for $c/a < 1.07$ in PZT films grown on STO as was observed in Fig. 2.

The Rayleigh relations are frequently employed to study the extrinsic contributions due to defects of the dielectric response in ferroelectric films.[21,22] In this analysis, the dependence of the dielectric constant on the sub-coercive AC electric field excitation E_0 is studied using the following relation:

$$\varepsilon_r - \varepsilon_r^0 = \alpha E_0, \tag{1}$$

where ε_r^0 and α are the intrinsic component of the dielectric constant and the Ralyleigh coefficient, respectively. α is a measure of the extrinsic contributions to the dielectric properties. The larger the value of α, the more dominant the effects of defects on the overall electrical properties of the film. Fig. 3(e) plots $\varepsilon_r - \varepsilon_r^0$ as a function of E_0 for the PZT samples at 100 kHz. It is clear that ε_r is more sensitive to the AC electric field excitation in the relaxed PZT film than in the strained ones. Fig. 3(e) shows the variation of α/ε_r as a function of tetragonality. We observe in Fig. 3(e) that α/ε_r is almost an order of magnitude higher in the relaxed PZT films compared to that in strained films.

Previous studies on the effects of strain relaxation in PZT films showed that the remnant polarization and the phase transition temperature depend weakly of the strain state of the film.[14,15] On the other hand, our results indicate that the dielectric properties of ferroelectric films are more strongly affected by extrinsic mechanisms such defects and dislocations. Given that strain relaxation plays an important role in the fatigue mechanism of epitaxial ferroelectric thin films,[7] similar dielectric characterization can provide useful insights in the study of fatigue.

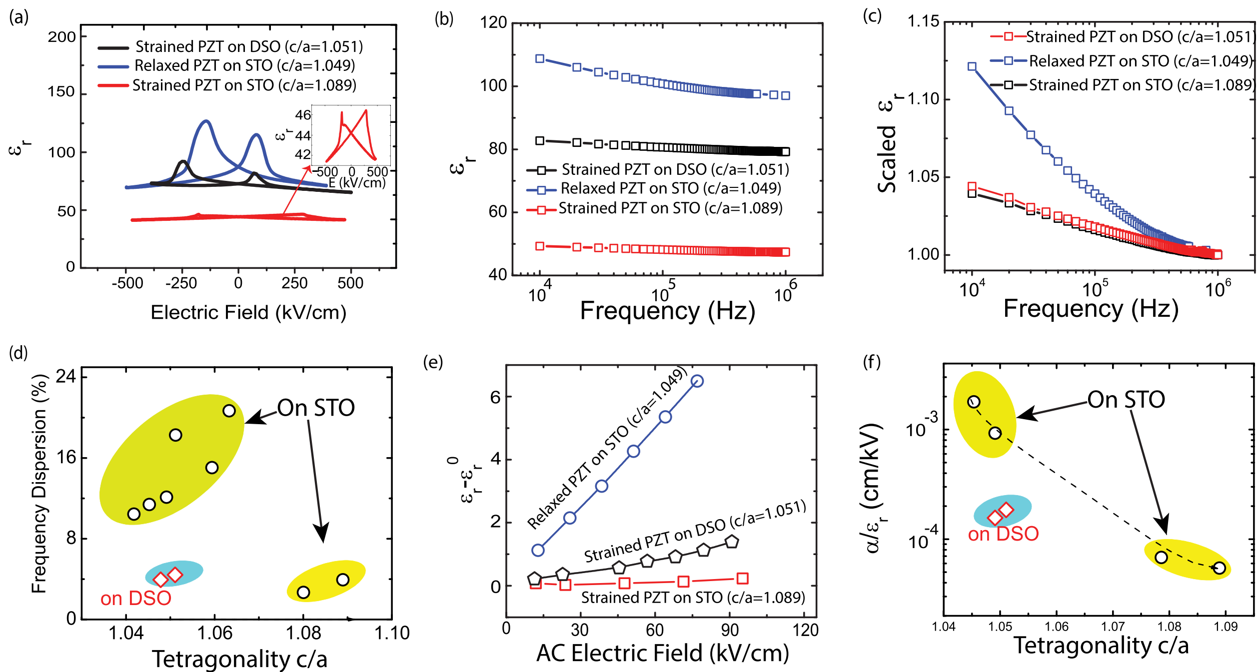

FIG. 3. (a) Comparison of dielectric constant (ε_r)-electric field characteristics of strained PZT films grown on STO and DSO substrates and a relaxed PZT film grown on STO substrate. (b) and (c) Dielectric constant (b) and scaled dielectric constant (c) as functions of the frequency. (d) Frequency dispersion of the PZT films as a function of the tetragonality c/a. (e) Comparison of ($\varepsilon_r - \varepsilon_{r,0}$)-AC electric field characteristics of strained PZT films grown on STO and DSO substrates and a relaxed PZT film grown on STO substrate. (f) α/ε_r of PZT samples as a function of tetragonality c/a.

In summary, we have studied the correlation between the structural and the dielectric properties in a set of 40 nm PZT films that are either strained or relaxed to the misfit substrates. A large increase in defect and dislocation density due to strain relaxation is observed in epitaxial PZT films with tetragonality $c/a < 1.07$ grown on STO substrates, which results in a significant frequency dispersion of the dielectric constant and a strong Rayleigh type behavior in those samples. For a given combination of a ferroelectric thin film and a substrate, tetragonality c/a is a quantitative measure of the degree to which epitaxial strain has been relaxed in the film and the extent of extrinsic contributions to the dielectric properties can be predicted from the value of c/a.

This work was supported in part by FCRP (MSD) Center, STARNET LEAST Center, NSF E3S Center and Office of Naval Research (ONR). A.I.K. acknowledges the Qualcomm Innovation Fellowship 2012-13. The authors thank R. Ramesh, J. Clarkson, and C. Rayan for fruitful discussions.

[1]N. A. Pertsev, A. G. Zembilgotov, and A. G. Tagantsev, Phys. Rev. Lett. **80**, 1988 (1998).
[2]K. J. Choi, M. Biegalski, Y. L. Li, A. Sharan, J. Schubert, R. Uecker, P. Reiche, Y. B. Chen, X. Q. Pan, V. Gopalan, L.-Q. Chen, D. G. Schlom, and C. B. Eom, Science **306**, 1005 (2004).
[3]J. H. Haeni, P. Irvin, W. Chang, R. Uecker, P. Reiche, Y. L. Li, S. Choudhury, W. Tian, M. E. Hawley, B. Craigo, A. K. Tagantsev, X. Q. Pan, S. K. Streiffer, L. Q. Chen, S. W. Kirchoefer, J. Levy, and D. G. Schlom, Nature **430**, 758 (2004).
[4]R. J. Zeches, M. D. Rossell, J. X. Zhang, A. J. Hatt, Q. He, C.-H. Yang, A. Kumar, C. H. Wang, A. Melville, C. Adamo, G. Sheng, Y.-H. Chu, J. F. Ihlefeld, R. Erni, C. Ederer, V. Gopalan, L. Q. Chen, D. G. Schlom, N. A. Spaldin, L. W. Martin, and R. Ramesh, Science **326**, 977 (2009).
[5]J. H. Lee, L. Fang, E. Vlahos, X. Ke, Y. W. Jung, L. F. Kourkoutis, J.-W. Kim, P. J. Ryan, T. Heeg, M. Roeckerath, V. Goian, M. Bernhagen, R. Uecker, P. C. Hammel, K. M. Rabe, S. Kamba, J. Schubert, J. W. Freeland, D. A. Muller, C. J. Fennie, P. Schiffer, V. Gopalan, E. Johnston-Halperin, and D. G. Schlom, Nature **466**, 954 (2010).
[6]J. W. Matthews and A. E. Blakeslee, J. Cryst. Growth **27**, 118 (1974).
[7]D.-H. Do, P. G. Evans, E. D. Isaacs, D. M. Kim, C.-B. Eom, and E. M. Dufresne, Nature Mater. **3**, 365 (2004).
[8]M.-W. Chu, I. Szafraniak, R. Scholz, C. Harnagea, D. Hesse, M. Alexe, and U. Gosele, Nature Mater. **3**, 87 (2004).
[9]C. L. Canedy, H. Li, S. P. Alpay, L. Salamanca-Riba, A. L. Roytburd, and R. Ramesh, Appl. Phys. Lett. **77**, 1695 (2000).
[10]V. Nagarajan, C. L. Jia, H. Kohlstedt, R. Waser, I. B. Misirlioglu, S. P. Alpay, and R. Ramesh, Appl. Phys. Lett. **86**, 192910 (2005).
[11]H. P. Sun, W. Tian, X. Q. Pan, J. H. Haeni, and D. G. Schlom, Appl. Phys. Lett. **84**, 3298 (2004).
[12]Y. L. Li, S. Y. Hu, S. Choudhury, M. I. Baskes, A. Saxena, T. Lookman, Q. X. Jia, D. G. Schlom, and L. Q. Chen, J. Appl. Phys. **104k**, 104110 (2008).
[13]I. B. Misirlioglu, A. L. Vasiliev, S. P. Alpay, M. Aindow, and R. Ramesh, J. Mater. Sci. **41**, 697 (2006).
[14]H. N. Lee, S. M. Nakhmanson, M. F. Chisholm, H. M. Christen, K. M. Rabe, and D. Vanderbilt, Phys. Rev. Lett. **98**, 217602 (2007).
[15]S. Gariglio, N. Stucki, J.-M. Triscone, and G. Triscone, Appl. Phys. Lett. **90**, 202905 (2007).
[16]D. C. Houghton, D. D. Perovic, J.-M. Baribeau, and G. C. Weatherly, J. Appl. Phys. **67**, 1850 (1990).
[17]Y. Lin, C. Dai, Y. R. Li, X. Chen, C. L. Chen, A. Bhalla, and Q. X. Jia, Appl. Phys. Lett. **96**, 102901 (2010).
[18]V. Nagarajan, J. Junquera, J. Q. He, C. L. Jia, R. Waser, K. Lee, Y. K. Kim, S. Baik, T. Zhao, R. Ramesh, and Ph. Ghosez *et al.*, J. Appl. Phys. **100**, 051609 (2006).
[19]S. Mathews, R. Ramesh, T. Venkatesan, and J. Benedetto, Science **276**, 238 (1997).
[20]A. Sambri, D. Isarakorn, A. Torres-Pardo, S. Gariglio, P. Janphuang, D. Briand, O. Stephan, J. W. Reiner, J.-M. Triscone, N. F. de Rooij *et al.*, Smart Mater. Res. **2012**, 426048.
[21]R. E. Eitel, T. R. Shrout, and C. A. Randall, J. Appl. Phys. **99**, 124110 (2006).
[22]A. K. Tagantsev, I. Stolichnov, E. L. Colla, and N. Setter, J. Appl. Phys. **90**, 1387 (2001).